



Effect of Variable Gravity on Darcy Flow with Impressed Horizontal Gradient and Viscous Dissipation

K. Roy[†] and P. Murthy

Department of Mathematics, Indian Institute of Technology Kharagpur, Kharagpur 721302, W. B., India

[†] *Corresponding Author Email: komolika.roy89@gmail.com*

(Received September 16, 2015; accepted December 8, 2015)

ABSTRACT

The effect of variable gravity on the free convection in a horizontal porous layer with viscous dissipation is investigated. The bottom boundary is taken as adiabatic and there is a non-uniform temperature distribution along the upper boundary. The effect of viscous dissipation is significant and the top boundary temperature distribution is assumed to have a constant gradient. The gravity varies linearly with the height. A linear stability analysis of the basic flow is carried out. The critical horizontal Rayleigh number is calculated for oblique roll disturbances. The longitudinal rolls are found to be the most unstable ones. The viscous dissipation has a destabilizing effect. There is a drastic decrease in the value of critical horizontal Rayleigh number when modified variable gravity parameter changes from -1 to 1 .

Keywords: Darcy flow; Variable gravity; Viscous dissipation.

NOMENCLATURE

a	non-dimensional wave number		disturbance (U, V, W)
c	heat capacity per unit mass	(x, y, z)	non-dimensional coordinates
$f(z), h(z)$	eigen functions		
g_0	modulus of the reference gravitational acceleration	α	thermal diffusivity
\mathbf{g}	gravitational acceleration	β	volumetric coefficient of thermal expansion
Ge	Gebhart number	η	variable gravity parameter
k	thermal conductivity	$\tilde{\eta}$	real exponential coefficient $\Re(\lambda)$
\hat{k}	unit vector in z -direction	Θ	non-dimensional temperature disturbance
K	permeability	λ	complex exponential coefficient, $\tilde{\eta} + i\tilde{\omega}$
L	thickness of the layer	μ	dynamic viscosity
p	non-dimensional pressure	ν	kinematic viscosity
P	non-dimensional pressure disturbance	ξ	complex parameter
q_h	horizontal heat flux	ρ	fluid density at $\bar{T} = \bar{T}_0$
Ra	horizontal Darcy-Rayleigh number	σ	heat capacity ratio
t	non-dimensional time	χ	inclination angle of the oblique rolls
T	non-dimensional temperature	Ψ	streamfunction
\hat{T}_B	reduced non-dimensional temperature	$\tilde{\omega}$	imaginary exponential coefficient
\bar{T}_0	reference temperature		$\Im(\lambda)$
\mathbf{u}	non-dimensional velocity vector (u, v, w)		
\mathbf{U}	non-dimensional velocity		

1. INTRODUCTION

The problem of convection in porous media is of a great interest among the researchers be-

cause of its wide range of applications from engineering to geophysical problems. In most of the earlier studies of convection in porous media, the contribution of the viscous dissipa-

tion to the energy equation has been neglected. However, in recent years it has been noted that in mixed convection and vigorous natural convection flows in porous media, viscous dissipation may become more significant. Also gravity has been assumed to be constant in most of the experimental and theoretical studies. But this assumption may not give accurate result while considering large scale flows, *e.g.* flows in ocean, atmosphere or earth's mantle, because the gravity field is varying with height from earth's surface. In this cases considering gravity as variable will help one to produce more accurate results. The convection of a fluid through a flat layer bounded above and below by perfectly conducting media with vertical temperature gradient is considered by Horton and Rogers (1945). The instability of a horizontal fluid layer where the gravitational field is varying with height is investigated by Pradhan and Samal (1987). Later Straughan (1989) done the linear instability and non-linear energy stability analysis for convection in a horizontal porous layer with variable gravity effect. Alex *et al.* (2001) investigated the effect of variable gravity on the onset of convection in an isotropic porous medium with internal heat source and inclined temperature gradient. The effect of variable gravity field on the onset of thermosolutal convection in a fluid saturated isotropic porous layer is studied by Alex and Patil (2001). Barletta *et al.* (2009) considered a horizontal porous layer with an adiabatic lower boundary and an isothermal upper boundary and discussed the effect of viscous dissipation on parallel Darcy flow by means of linear stability analysis. The effect of viscous dissipation, on the stability of flow in a porous layer with an adiabatic bottom boundary and a top boundary with a stationary and non-uniform temperature distribution is investigated by Barletta *et al.* (2010). The linear thermoconvective instability of a parallel flow in a horizontal porous layer bounded by impermeable walls and subject to a uniform heat flux is studied by Barletta (2012). Roy and Murthy (2015) discussed the effect of Soret parameter on double diffusive convection when the convection occurs solely due to viscous dissipation. Recently the problem of convection in porous media with internal heat source and variable gravity effect is studied using three-dimensional simulations (Harfash 2014). In this study the effect of variable gravity on convection in porous media with an adiabatic lower boundary and an upper boundary with a horizontal temperature gradient is analyzed by the means of linear stability analysis. The viscous dissipation is non-negligible. It is assumed that

the gravity varies linearly with height.

2. MATHEMATICAL FORMULATION

A porous slab of height L bounded by two horizontal impermeable planes $\bar{z} = 0$ and $\bar{z} = L$ is considered. The gravity vector \mathbf{g} is varying linearly with \bar{z} (Chen and Chen 1992) so that $\mathbf{g} = -g_0(1 + \bar{\eta} \bar{z})\hat{\mathbf{k}}$, where $\bar{\eta}$ is the variable gravity parameter which is assumed to be constant. The bottom boundary is adiabatic. There is a linear change in temperature in the horizontal \bar{x} -direction along the upper boundary (as indicated in the Eq. 5). Here 'bar' denotes dimensional quantities.

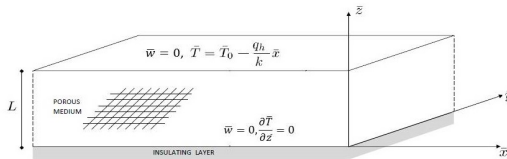


Fig. 1. The physical system and the boundary conditions

With the Oberbeck-Boussinesq approximation, the governing equations for the Darcy flow can be written as $\bar{\nabla} \cdot \bar{\mathbf{u}} = 0$ (1)

$$\frac{\mu}{K} \bar{\mathbf{u}} = -\bar{\nabla} \bar{p} + \rho_0 g_0 (1 + \bar{\eta} \bar{z}) \beta (\bar{T} - \bar{T}_0) \hat{\mathbf{k}} \quad (2)$$

$$\sigma \frac{\partial \bar{T}}{\partial t} + \bar{\mathbf{u}} \cdot \bar{\nabla} \bar{T} = \alpha \bar{\nabla}^2 \bar{T} + \frac{\nu}{Kc} \bar{\mathbf{u}} \cdot \bar{\mathbf{u}} \quad (3)$$

The boundary conditions are

$$\bar{z} = 0 : \quad \bar{w} = 0, \quad \frac{\partial \bar{T}}{\partial \bar{z}} = 0, \quad (4)$$

$$\bar{z} = L : \quad \bar{w} = 0, \quad \bar{T} = \bar{T}_0 - \frac{q_h}{k} \bar{x} \quad (5)$$

While writing the governing equations, the effect of viscous dissipation to the energy equation is considered and the fluid and solid are assumed to be in local thermal equilibrium. The last term in Eq. 3 represents the effect of viscous dissipation for the Darcy flow. A detailed study for deriving the expression for viscous dissipation is given in Bejan (2013), Murthy and Singh (1997).

The governing equations are non-dimensionalized using the following non-dimensional parameters.

$$(\bar{x}, \bar{y}, \bar{z}) = (x, y, z)L, \quad (\bar{u}, \bar{v}, \bar{w}) = (u, v, w) \frac{\alpha}{L}, \quad \eta = \bar{\eta}L, \\ \bar{T} = \bar{T}_0 + T \frac{\nu \alpha}{g_0 \beta L K}, \quad \bar{t} = t \frac{\sigma L^2}{\alpha}, \quad \bar{p} = p \frac{\mu \alpha}{K} \quad (6)$$

The non-dimensional formulation of the problem is given by

$$\nabla \cdot \mathbf{u} = 0 \tag{7}$$

$$\mathbf{u} = -\nabla p + (1 + \eta z)T\hat{\mathbf{k}} \tag{8}$$

$$\frac{\partial T}{\partial t} + \mathbf{u} \cdot \nabla T = \nabla^2 T + Ge\mathbf{u} \cdot \mathbf{u} \tag{9}$$

$$z = 0 : \quad w = 0, \quad \frac{\partial T}{\partial z} = 0, \tag{10}$$

$$z = 1 : \quad w = 0, \quad T = -Rax \tag{11}$$

where the non-dimensional parameters are

$$Ge = \frac{\beta g_0 L}{c}, \quad Ra = \frac{\beta g_0 q_h K L^2}{\nu \alpha k} \tag{12}$$

2.1 Steady State Solution

Let us assume the velocity, temperature and pressure for the basic flow is given by

$$\begin{aligned} u_B &= u_B(z), & v_B &= w_B = 0, \\ T_B &= T_B(x, z), & p_B &= p_B(x, z) \end{aligned} \tag{13}$$

After solving Eqs. (7)-(11) for u_B , T_B and p_B , we get,

$$u_B(z) = Raz(1 + \eta z) \tag{14}$$

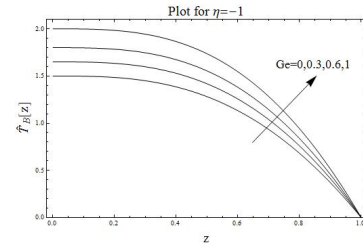
$$\begin{aligned} T_B(x, z) &= -Rax + \frac{Ra^2}{120} [5\{4(1 - z^3) + \eta(1 - z^4)\} \\ &\quad + Ge\{10(1 - z^4) + 6\eta(1 - z^5) + \eta^2(1 - z^6)\}] \end{aligned} \tag{15}$$

$$\begin{aligned} p_B(x, z) &= -Raxz(1 + \frac{\eta z}{2}) - \frac{Ra^2 z}{2880} [20\{6z^3 + 6z^4\eta + \\ &\quad z^5\eta^2 - 6(4 + \eta) - 3z\eta(4 + \eta)\} + Ge\{48z^4 + \\ &\quad 64z^5\eta + 24z^6\eta^2 + 3z^7\eta^3 - 24(10 + 6\eta + \\ &\quad \eta^2) - 12z\eta(10 + 6\eta + \eta^2)\}] \end{aligned} \tag{16}$$

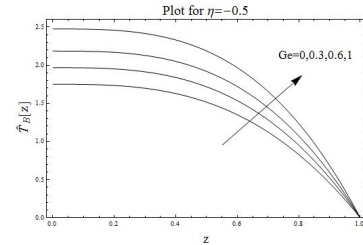
To analyze the behavior of the basic temperature profile, we introduce a reduced temperature gradient

$$\begin{aligned} \hat{T}_B(z) &= \frac{12}{Ra^2} [T_b(x, z) + Rax] \\ &= \frac{1}{10} [5\{4(1 - z^3) + \eta(1 - z^4)\} + Ge\{10(1 - z^4) \\ &\quad + 6\eta(1 - z^5) + \eta^2(1 - z^6)\}] \end{aligned} \tag{17}$$

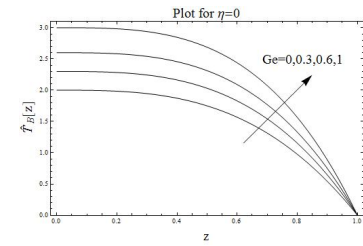
Plots of this reduced temperature functions for different values of η are given in Fig. 2. From these figures, it can be seen that the temperature at the lower boundary is always greater than the temperature at the upper boundary when x is constant. When Ge is constant, the temperature at the lower boundary increases as η increases from -1 to 1 .



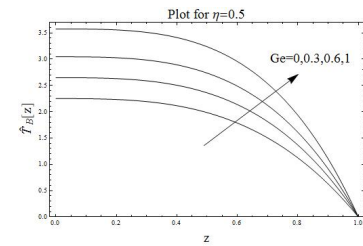
(a) $\eta = -1$



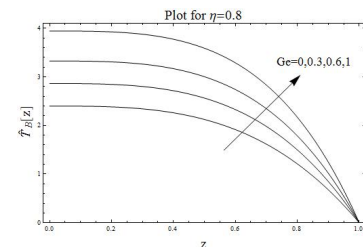
(b) $\eta = -0.5$



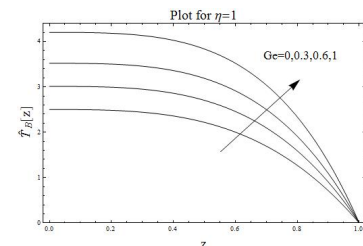
(c) $\eta = 0$



(d) $\eta = 0.5$



(e) $\eta = 0.8$



(f) $\eta = 1$

Fig. 2. $\hat{T}_B[z]$ vs. z for different values of η .

2.2 Linear Stability Analysis

Using small perturbation parameter ϵ , the basic solutions are perturbed. Linearizing Eqs. (7)-(11) with respect to ϵ , we get the linearized system of governing equations as

$$\nabla \cdot \mathbf{U} = 0 \quad (18)$$

$$\mathbf{U} = -\nabla P + (1 + \eta z)\theta \hat{\mathbf{k}} \quad (19)$$

$$\begin{aligned} \frac{\partial \theta}{\partial t} + u_B \frac{\partial \theta}{\partial x} + U \frac{\partial T_B}{\partial x} + W \frac{\partial T_B}{\partial z} \\ = \nabla^2 \theta + 2Geu_B U \end{aligned} \quad (20)$$

$$z = 0 : \quad W = 0, \quad \frac{\partial \theta}{\partial z} = 0 \quad (21)$$

$$z = 1 : \quad W = 0, \quad \theta = 0 \quad (22)$$

The pressure-temperature formulation of the governing equations is given by

$$\nabla^2 P = (1 + \eta z) \frac{\partial \theta}{\partial z} + \theta \eta \quad (23)$$

$$\begin{aligned} \frac{\partial \theta}{\partial t} + u_B \frac{\partial \theta}{\partial x} - \frac{\partial P}{\partial x} \frac{\partial T_B}{\partial x} - \left(\frac{\partial P}{\partial z} - (1 + \eta z)\theta \right) \frac{\partial T_B}{\partial z} \\ = \nabla^2 \theta - 2Geu_B \frac{\partial P}{\partial x} \end{aligned} \quad (24)$$

$$z = 0 : \quad \frac{\partial P}{\partial z} = \theta, \quad \frac{\partial \theta}{\partial z} = 0 \quad (25)$$

$$z = 1 : \quad \frac{\partial P}{\partial z} = 0, \quad \theta = 0 \quad (26)$$

The plane wave solutions of Eqs. (23)-(26) in the form of plane waves which are inclined with respect to x-axis is assumed (Barletta *et al.* 2010). For neutral stability Eqs.(23)-(26) can be written as

$$f'' - a^2 f - (1 + \eta z)h' - h\eta = 0 \quad (27)$$

$$\begin{aligned} h'' - \left[a^2 - \frac{Ra^2}{120}(1 + \eta z)[5(12z^2 + 4z^3\eta) + Ge(40z^3 + 30z^4\eta + 6z^5\eta^2)] + i(\tilde{\omega} + a \cos \chi Ra z \right. \\ \left. \left(1 + \frac{\eta z}{2}\right)\right] h - \frac{Ra^2 z^2}{120}[5(12 + 4z\eta) + Ge(40z + 30z^2\eta + 6z^3\eta^2)]f' - ia \cos \chi Ra(1 + 2Gez \\ \left. \left(1 + \frac{\eta z}{2}\right)\right) f = 0 \end{aligned} \quad (28)$$

$$z = 0 : \quad f' = h, \quad h' = 0, \quad (29)$$

$$z = 1 : \quad f' = 0, \quad h = 0 \quad (30)$$

Here χ is the inclination angle between the direction of the basic flow and the propagation direction of the disturbance wave. For $\chi = \frac{\pi}{2}$, the disturbance will produce longitudinal rolls and for $\chi = 0$ we get transverse rolls. Critical Rayleigh number is obtained for stationary longitudinal modes and oblique rolls. For stationary longitudinal rolls $\lambda = 0$ i.e. $\tilde{\eta} = 0$ and $\tilde{\omega} = 0$

2.3 Numerical Solution of the Eigenvalue Problem

The eigen value problem given by Eqs. (27)-(30) is solved numerically by a fourth order Runge-Kutta method accompanied by shooting method (Barletta *et al.* 2010). The new set of initial conditions is

$$z = 0 : \quad f = \xi, \quad f' = 1, \quad h = 1, \quad h' = 0 \quad (31)$$

For a set of input parameters (a, Ge, η), using the boundary conditions at $z = 1$ one can calculate the values of $(Ra, \tilde{\omega})$ and also ξ_r, ξ_i , where $\xi = \xi_r + i\xi_i$. We have solved the problem in *Mathematica 8* using *NDSolve* and *FindRoot*. After getting Ra for a given pair (a, Ge, η) , the critical horizontal Rayleigh number (Ra_{cr}) is obtained by minimizing $Ra(a)$ for every (Ge, η) i.e. $Ra_{cr} = \min[Ra(a)]$. While applying shooting method, the initial guess for $(Ra, \tilde{\omega})$ plays an important role as the convergence of the method depends on this initial guess. For longitudinal rolls, an initial guess can be found by Galerkin's method of weighted residuals.

3. ANALYTICAL SOLUTION

An approximate solution of Eqs. (18)-(22) can be found for longitudinal rolls by Galerkin's method of weighted residuals (Finlayson and Scriven 1966; Barletta *et al.* 2010). The weighted residual method yields expression for Ra .

$$\begin{aligned} Ra^2 = \frac{2187\pi^8}{256a^2(3\pi + 4\eta)} [-960Ge\pi^2 - 252\pi^3 + \\ 108\pi^4 + 108Ge\pi^4 + 5856Ge\pi\eta - 480\pi^2\eta - \\ 2880Ge\pi^2\eta + 54\pi^4\eta + 11648Ge\eta^2 - \\ 1440Ge\pi^2\eta^2 + 27Ge\pi^4\eta^2]^{-1} (4a^4 + \\ 5a^2\pi^2 + \pi^4) \end{aligned} \quad (32)$$

Now to get the critical value of Ra , we minimize the right hand side of Eq.(32) with respect to a .

This gives the critical values

$$a_{cr} = \frac{\pi}{\sqrt{2}}$$

$$Ra_{cr}^2 = \frac{19683\pi^{10}}{256(3\pi + 4\eta)} [6\pi^2(-42\pi - 80\eta + 9\pi^2(2 + \eta)) + Ge(5856\pi\eta + 11648\eta^2 + 27\pi^4(2 + \eta^2) - 480\pi^2(2 + 6\eta + 3\eta^2))]^{-1} \quad (33)$$

Table 1 Comparison of critical horizontal Rayleigh number vs Ge for longitudinal rolls when $\eta = 0$

Ge	Barletta <i>et al.</i> (2010)		Present Results	
	Ra_{cr}	a_{cr}	Ra_{cr}	a_{cr}
0	15.0311	2.62247	15.0310	2.62351
0.2	14.4496	2.63512	14.4495	2.63603
0.4	13.9300	2.64636	13.9300	2.64637
0.6	13.4622	2.65639	13.4622	2.65636
0.8	13.0382	2.66540	13.0382	2.66545
1	12.6516	2.67354	12.6516	2.67344

Table 2 Critical horizontal Rayleigh number and critical wave number for different values of Ge and η for longitudinal rolls

(a) $\eta = 0.5$

Ge	Ra_{cr}	a_{cr}
0	12.6539	2.72423
0.1	12.3605	2.73331
0.5	11.3607	2.76396
1	10.3941	2.79286

(b) $\eta = 1$

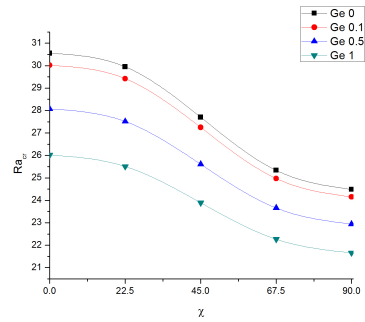
Ge	Ra_{cr}	a_{cr}
0	10.9456	2.79457
0.1	10.6557	2.80689
0.5	9.68795	2.84774
1	8.77982	2.88532

(c) $\eta = -0.5$

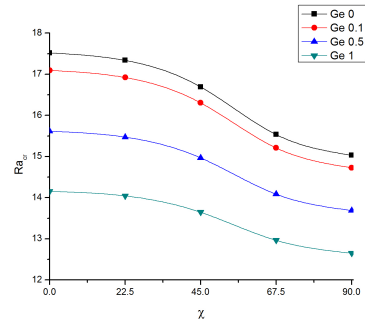
Ge	Ra_{cr}	a_{cr}
0	18.5734	2.45527
0.1	18.2634	2.45813
0.5	17.1614	2.46825
1	16.0269	2.53359

(d) $\eta = -1$

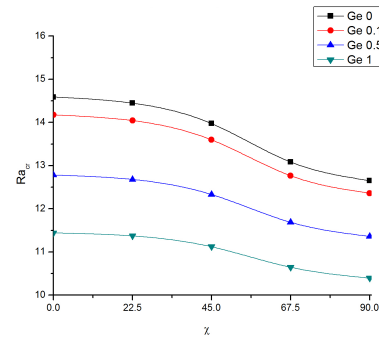
Ge	Ra_{cr}	a_{cr}
0	24.4848	2.30665
0.1	24.1520	2.30718
0.5	22.9442	2.30910
1	21.6611	2.31117



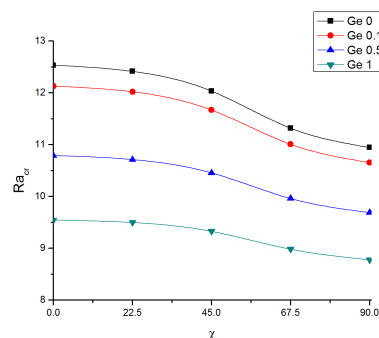
(a) $\eta = -1$



(b) $\eta = 0$



(c) $\eta = 0.5$



(d) $\eta = 1$

Fig. 3. The dependence of Ra_{cr} on χ for different values of Ge and η .

4. RESULTS AND DISCUSSION

4.1 Longitudinal Rolls

A comparison of our results for $\eta = 0$ and the results obtained by Barletta *et al.* (2010) are

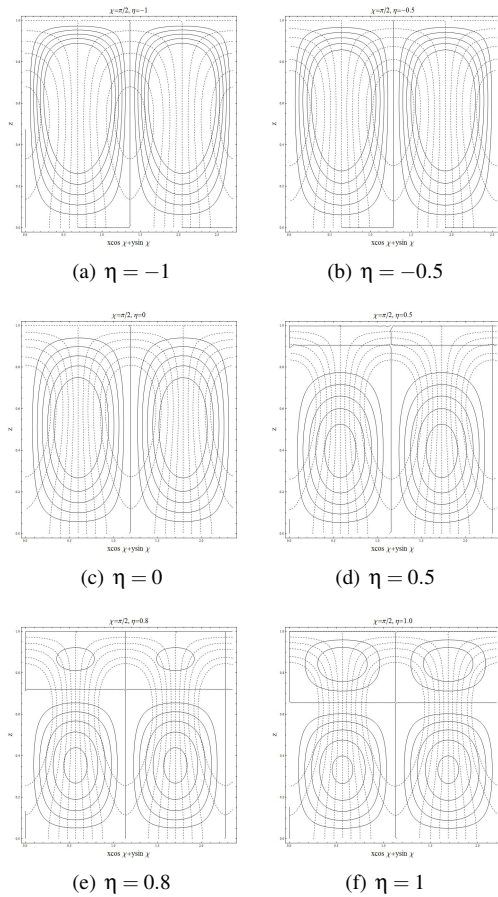


Fig. 4. Streamlines (solid lines) and isotherms (dashed lines) for $a = a_{cr}$, $Ra = Ra_{cr}$, $Ge = 0$, $t = 0$, $\chi = \frac{\pi}{2}$ with different values of η .

given in Table 1. Table 2 shows the values of Ra_{cr} and a_{cr} for different values of Ge and η for longitudinal rolls. From Table 1 and Table 2, it is clear that when η decreases from 0 and becomes negative *i.e.* the gravitational field decreases with height, the Rayleigh number increases and this results in a more stable flow. When η increases from 0 *i.e.* the gravitational field increases with height, the Rayleigh number decreases resulting in a more unstable flow.

4.2 Oblique Rolls for Different Values of η

The dependence of Ra_{cr} on χ (when Ge and η are constant) is displayed in Fig. 3.

It shows that for all values of Ge and η , Ra_{cr} decreases as χ increases from 0 to $\pi/2$. It is concluded that longitudinal rolls are most unstable. For oblique rolls also Ra_{cr} increases when gravitational field decreases with height from its reference value (η decreases from 0) and Ra_{cr} decreases as gravitational field increases with height (η increases from 0). This proves that in-

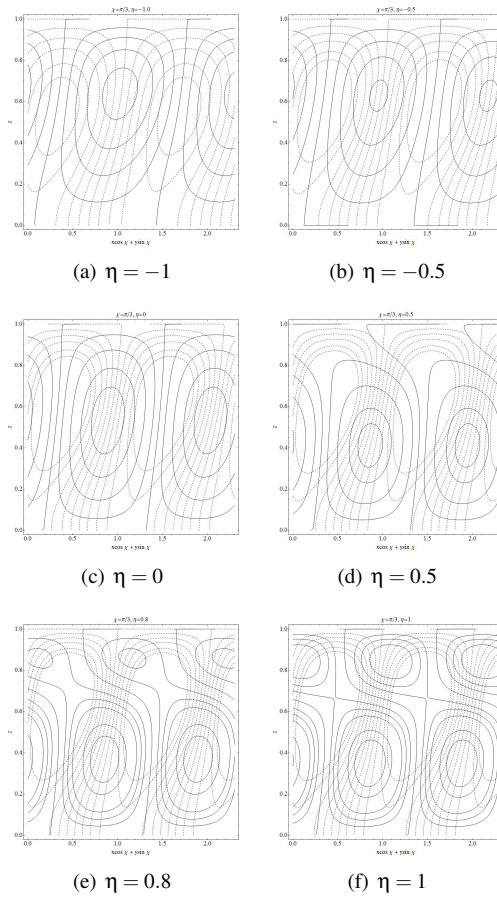


Fig. 5. Streamlines (solid lines) and isotherms (dashed lines) for $a = a_{cr}$, $Ra = Ra_{cr}$, $Ge = 0$, $t = 0$, $\chi = \frac{\pi}{3}$ with different values of η .

creasing gravitational acceleration advances the onset of convection. From these results, it is evident that viscous dissipation has a destabilizing effect on convection both in presence and in absence of variable gravity field.

4.3 Convective Roll Patterns for $Ge=0$ and Different Values of η

The streamlines $\psi = constant$ (solid lines) and isotherms $\theta = constant$ (dashed lines) corresponding to the critical conditions for $Ge = 0$ with different values of η and χ are represented in Figs (4)-(7).

When η is constant, there is a clear bending of convective rolls as χ decreases from $\frac{\pi}{2}$ to 0. Also, when χ is constant and η decreases from 0, the streamlines are magnified, but the isotherms are shrunken. But as η increases from 0, the unicellular streamlines tend to become bi-cellular and the isotherms are magnified. The shape of the convective rolls are not much affected by the viscous dissipation.

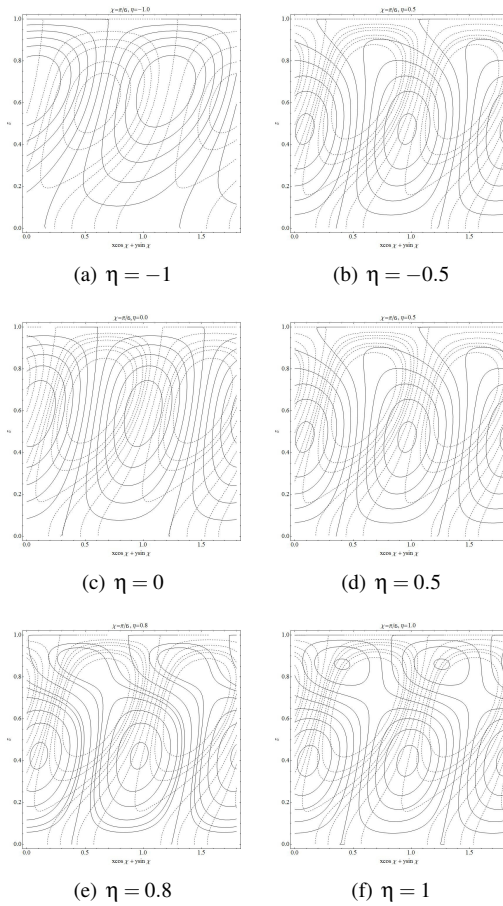


Fig. 6. Streamlines(solid lines) and isotherms (dashed lines) for $a = a_{cr}$, $Ra = Ra_{cr}$, $Ge = 0$, $t = 0$, $\chi = \frac{\pi}{6}$ with different values of η .

5. CONCLUSIONS

The effect of variable gravity on parallel Darcy flow in a horizontal plane porous layer with impermeable boundaries has been studied. The effect of viscous dissipation to the energy equation is taken into account. In the existing literature although gravity is considered as variable, viscous dissipation effect is neglected. Here we have discussed the effect of variable gravity when the viscous dissipation effect is significant. It has been seen that for constant Gebhart number, the basic temperature at the lower boundary increases as variable gravity parameter η increases from -1 to 1 . It is observed that for a constant η , Ra_{cr} is a decreasing function of Ge . This proves that viscous dissipation has a destabilizing effect. When Ge is constant, Ra_{cr} decreases when gravitational acceleration increases with height from its reference value (η increases from 0 to 1) and an opposite effect is seen when η decreases from 0 . This shows that the flow tends to be more unstable if g increases

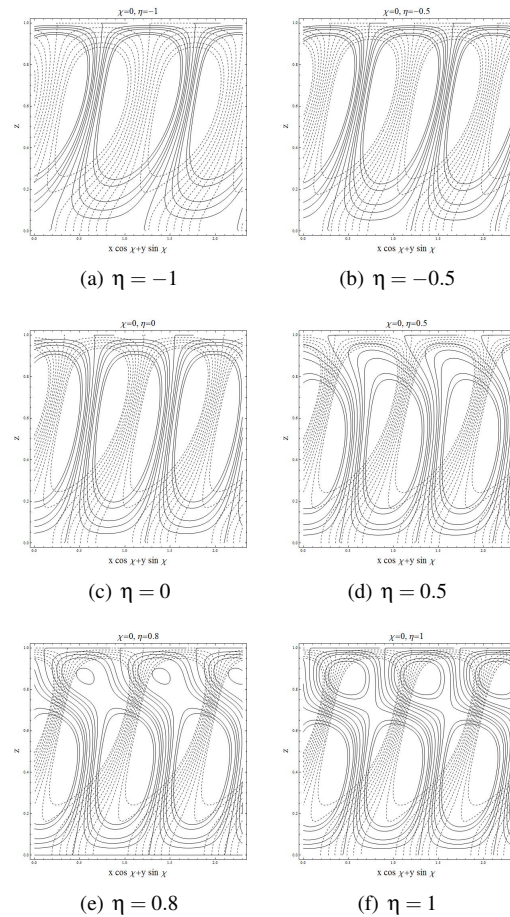


Fig. 7. Streamlines (solid lines) and isotherms (dashed lines) for $a = a_{cr}$, $Ra = Ra_{cr}$, $Ge = 0$, $t = 0$, $\chi = 0$ with different values of η .

with height. The longitudinal rolls are happen to be the most unstable ones. The variable gravity has a significant effect on convective rolls. As η increases from 0 to 1 , i.e. if g increases with height, the unicellular streamlines tend to become bi-cellular.

REFERENCES

- Alex, S. and P. Patil (2001). Effect of variable gravity field on soret driven thermosolutal convection in a porous medium. *International communications in heat and mass transfer* 28(4), 509–518.
- Alex, S., P. Patil and K. Venkatakrishnan (2001). Variable gravity effects on thermal instability in a porous medium with internal heat source and inclined temperature gradient. *Fluid Dynamics Research* 29(1), 1–6.
- Barletta, A. (2012). Thermal instability in a horizontal porous channel with horizon-

- tal through flow and symmetric wall heat fluxes. *Transport in porous media* 92(2), 419–437.
- Barletta, A., M. Celli and D. Nield (2010). Unstably stratified Darcy flow with impressed horizontal temperature gradient, viscous dissipation and asymmetric thermal boundary conditions. *International Journal of Heat and Mass Transfer* 53(9), 1621–1627.
- Barletta, A., M. Celli and D. Rees (2009). The onset of convection in a porous layer induced by viscous dissipation: a linear stability analysis. *International Journal of Heat and Mass Transfer* 52(1), 337–344.
- Bejan, A. (2013). *Convection heat transfer*. John Wiley & Sons.
- Chen, C. and F. Chen (1992). Onset of salt finger convection in a gravity gradient. *Physics of Fluids A: Fluid Dynamics* 4, 451.
- Finlayson, B. and L. Scriven (1966). The method of weighted residuals a review. *Appl. Mech. Rev* 19(9), 735–748.
- Harfash, A. (2014). Three-dimensional simulations for convection in a porous medium with internal heat source and variable gravity effects. *Transport in Porous Media* 101(2), 281–297.
- Horton, C. and F. Rogers (1945). Convection currents in a porous medium. *Journal of Applied Physics* 16(6), 367–370.
- Murthy, P. and P. Singh (1997). Effect of viscous dissipation on a non-darcy natural convection regime. *International journal of heat and mass transfer* 40(6), 1251–1260.
- Pradhan, G. and P. Samal (1987). Thermal stability of a fluid layer under variable body forces. *Journal of Mathematical Analysis and Applications* 122(2), 487–495.
- Roy, K. and P. Murthy (2015). Soret effect on the double diffusive convection instability due to viscous dissipation in a horizontal porous channel. *International Journal of Heat and Mass Transfer* 91, 700–710.
- Straughan, B. (1989). Convection in a variable gravity field. *Journal of Mathematical Analysis and Applications* 140(2), 467–475.